ELPOA: data processing of chromatic differences of the tilt measured with a polychromatic laser guide star

Jérôme Vaillant, Eric Thiebaut, Michel Tallon

ELPOA: Data processing of chromatic differences of the tilt measured with a polychromatic laser guide star.

Jérôme Vaillant, Éric Thiébaut, Michel Tallon

Centre de Recherches Astronomiques de Lyon (CRAL),
Observatoire de Lyon, F-69561 Saint Genis Laval Cedex, France

ABSTRACT

In this paper we present an experiment for measuring the chromatic differences of the tilt used a for polychromatic laser guide star, a suitable solution to overcome the monochromatic laser guide star limitation: the tilt indetermination. A comparative study between two types of data processing is done: the classical estimation of angle of arrival by the image center of gravity, and a new one: an estimation of tilts by fitting a phase map in the polychromatic case. From these studies, expected precision is derived and comparison between simulations and data is done.

Keywords: Laser guide star, tilt indetermination, refractive air index, image processing, centroiding, wavefront estimation

1. INTRODUCTION: MEASURING THE CHROMATIC DIFFERENCES OF THE TILT

Measuring the chromatic differences of the tilt (also called differential tilt) is a corner stone of polychromatic laser guide star (henceforth PLGS). The PLGS, proposed by R.Foy et al. in 1995[1] is a suitable solution to the "tilt problem". By tilt problem we mean the impossibility of an adaptive optic system to sense the tilt (mean slope of the wavefront) from a monochromatic laser guide star.[2] This limitation has a great impact on sky coverage[3,4] (which is nearly null on the visible range). So finding a suitable solution to overcome this drawback of monochromatic laser guide stars has motivated many studies.[1,5–7]

Here we present our work about measuring the differential tilt, motivated by the fact that this measurement has never been done successfully up to day. Indeed, as we will see on the following, the differential tilt is tiny compared to the tilt so it is a right assumption to neglect it in adaptive optic systems. Nevertheless it is a key for solving tilt problem. Determination of the tilt from the differential tilt uses the air refractive index chromaticity associated with a polychromatic backscattering.[8] Applying the properties of air index variations with wavelength, the tilt can be estimated from the chromatic differences of the tilt using the formula[1]:

$$\theta_{\lambda_3} = \frac{n_{\lambda_3} - 1}{n_{\lambda_1} - n_{\lambda_2}} (\theta_{\lambda_1} - \theta_{\lambda_2}) \tag{1}$$

Where θ_λ and n_λ denote respectively the tilt and the air refractive index at the wavelength λ. It is important to note that this relation is valid not only for the tilt, but also for any mode or linear function of modes, except the piston (average of wavefront over the pupil), especially the angle of arrival. The smallness of the differential tilt lays on the factor $\Delta n/(n-1)$ which is less than $1/25$ for visible range (Δn denote the difference of air index). The differential tilt measurement requires a high quality measurement and an careful data processing as done in the MaTilD experiment to demonstrate its feasibility (see section 2). To achieve the best measurement as possible, we have developed two types of data processing: the usual image center of gravity to determine the angle of arrival, and a phase screen model fitting in polychromatic case to estimate the tilt mode; and for each one, we have estimated errors (see section 3). As a conclusion and based on previous estimations we compare simulation and real data results (see section 4).

2. MATILD: DESCRIPTION OF THE EXPERIMENTAL SETUP

The MaTilD experiment (which is the French achronim of "Differential Tilt Manipulation") was devised for demonstrating the feasibility of the differential tilt measurement and not for simulating for polychromatic laser star. So we choose to work in real conditions as best as possible. This mean a high flux, choice and monitoring of wavelengths, an optimal $D/r_0 \simeq 4$ as recommended by Fried,[9] a setup which avoid vibrations (equivalent to an achromatic tilt) easier than monitoring they, for instance with a pendular seismometer.[10] .

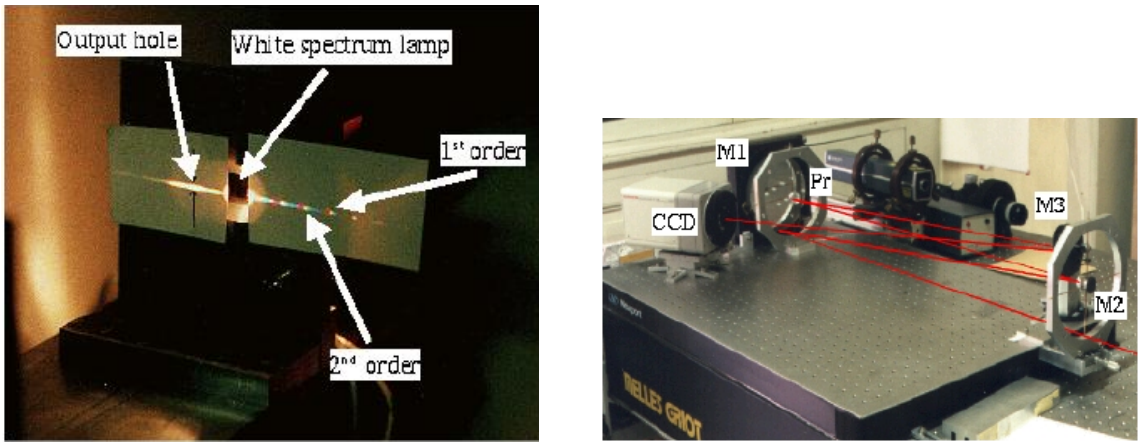

(a) Source of MaTilD

(b) Instrument of MaTilD

Figure 1. MaTilD: the multi-wavelength point-like source (a) is generated with an Échelle grating using the superposition of orders and the instrument (b) condense the beam (M1 and M2), disperse wavelengths (prism Pr) and make an image of the point source at each wavelengths with M3 on a CCD chip. During data acquisition, light coming for the source propagates trough 100m of turbulent atmosphere to the instrument, the beam is $3-16$m height (determining roughly the large scale of turbulence).

Under these constraints, the setup is the following: a horizontal propagation through the atmosphere, a point-like source with a discrete line spectrum and an instrument which separates wavelengths and make images of the point source (see figure 1). In each frame we have simultaneously, at each wavelength, the turbulence perturbed image of the point like source. As we take short exposure frames, the turbulence is frozen so there is a non-nil tilt which will be the same for all wavelengths except the expected differential tilt.

The primary mirror of the instrument has a diameter of 150mm which is a good trade-off between size and easiness of use considering, as shown by Fried, that the tilt excursion is maximized compared to image extension where $D/r_0 \simeq 4$. $r_0 = 3,5$cm is achieved at Lyon Observatory under standard turbulence with a 100m horizontal propagation.

The choice of wavelengths range is done considering the air index variation: the shorter and the more different the wavelengths are the bigger the differential tilt is (see air index curve in figure 2). Taking into account the efficiency of our CCD camera and optics transmission, the spectral range is 673nm $\rightarrow$ 337nm with four wavelengths in (673nm, 505nm, 404nm, 337nm). Distance between spots, on the CCD chip, have to be maximized to limit the effect of overlapping between monochromatic images. To allow different types of data processing we do not design an instrument too specific: images are sampled around Shannon frequency (equal at 500 nm). The scale is 0.33" per pixel and resulting in an under-sampling of 67% at the shortest wavelength (337nm). For the detector, a CCD chip of 512×512 pixels (pixel size 25μm) with a readout noise of 8 electrons is used. The dark current is totally negligible in short exposure images (20 ms). Data acquisition have been done during a clear winter night with a light wind and a r_0 of 4cm. 200 frames have been acquired and before processing they have been corrected for average dark and flat fields; typical frame looks like figure 3

3. DATA PROCESSING

In this part we consider two types of data processing to estimate the differential tilt: the usual one, computation of the center of gravity (see section 3.1) and a finer solution, the phase map fitting in polychromatic case (see section 3.2).

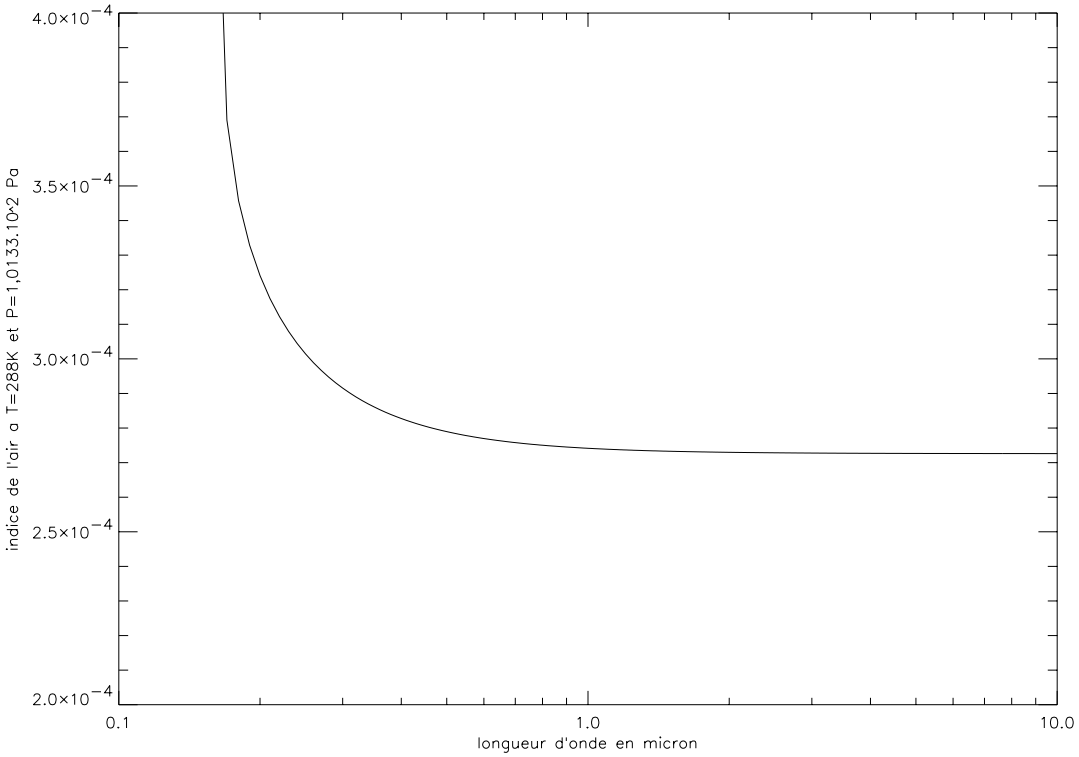

Figure 2. Air refractive index variation[11] with wavelength, in normal condition of pressure and temperature. Note that the difference of air index is bigger if wavelengths are more different and in the ultraviolet range.

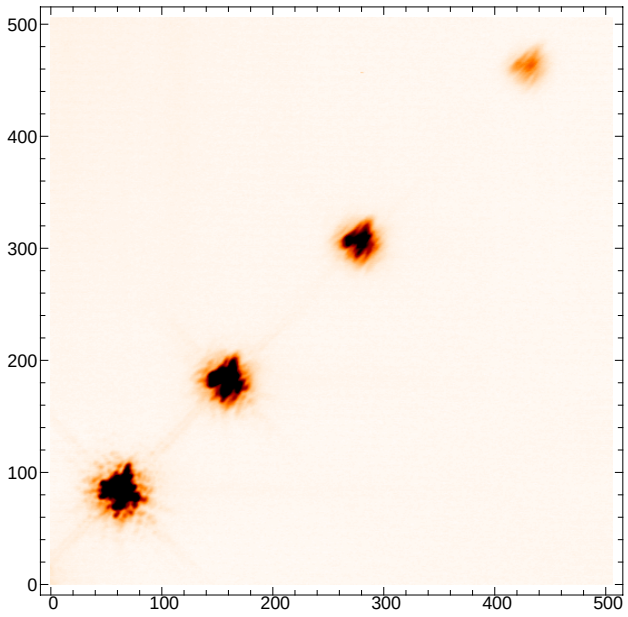

Figure 3. Typical frame obtained with the MaTilD experiment, from the bottom left corner to the top right corner wavelengths are: 673nm, 505nm, 404nm and 337nm

3.1. center of gravity

The center of gravity is largely used as an estimation of the tilt in Shark-Hartman detectors because it is a simple and fast technique. Despite it is an estimation of angle of arrival and not tilt*, as shown by Tatarskii,[12] we use it because the relation (1) is valid for tilt or angle of arrival. A great advantage of the center of gravity is that errors due to photon noise, sampling and CCD read-out noise can be estimated analytically as shown in the next three sections. But for other effects like windowing or image overlapping only simulation give an estimation of their impacts, because these noises are highly non-linear and turbulence dependent; this is done on the last section.

3.1.1. Effect of photon noise

The photon noise is due to the random nature of photons arrival which follow a Poisson law. This noise is always present and is the theoretical limitation because it can not be reduced by using better technology (as readout noise does for example). Its effect is studied by considering the center of gravity as the average of all photon positions x_i:

$$x_0 = \frac{1}{N_{ph}} \sum_i^{N_{ph}} x_i \tag{2}$$

This shows directly that the photon noise introduces no bias on the center of gravity estimation, but a noise. This noise, as a random error, can be characterized by its variance that is equal to the second order momentum of photon positions in image plane divided by the total number of detected photons:

$$\mathrm{Var}(\varepsilon_{\mathrm{ph}}) = \frac{M_2(x_i)}{N_{ph}} \tag{3}$$

Applying this relation for a Gaussian shaped image ($M_2(x_i) = \sigma^2_{\mathrm{image}}$, the variance of the Gaussian) we retrieve the well known standard deviation of photon noise error[13]: $\sigma_{\mathrm{image}}/\sqrt{N_{ph}}$.

3.1.2. Effect of spatial sampling

Now we consider the effect of the finite size of pixels. The photon position is not known with a precision better than the pixel size: information is lost about where the photon hits the CCD a pixel. To study this noise, let us note that the intensity given by the CCD is averaged over the pixel and that the center of gravity is the first order momentum of intensity. Using the properties of the Fourier transform relative to derivative and first order momentum of a function, we demonstrate that sampling introduce a bias:

$$\mathrm{B}_{\mathrm{sampling}} = \frac{\Delta x}{\pi} \sum_{k>0} \frac{(-1)^{k+1}\Delta x}{k} \Im[\hat{I}(\frac{k}{\Delta x})] \tag{4}$$

where Δx denotes the pixel size and $\Im[\hat{I}]$ the imaginary part of the intensity Fourier transform in image plane.

It is important to see that this bias is null as soon as the sampling frequency is greater than half of the Shannon frequency. This result from the representation of the center of gravity in Fourier space: it is the phase of the power spectral density at zero frequency. So aliasing is acceptable until it does not perturb the zero frequency: for the center of gravity estimation, we can under-sample with a factor 2 compared to Shannon sampling. Considering this, the number of pixels could be reduced by a factor 4 (for the point of view of sampling effect).

In the following we consider that we have no bias; this is the case in MaTilD experiment. Under this assumption we find the variance of the sampling error equal to:

$$\mathrm{Var}(\varepsilon_{\mathrm{sampling}}) = \frac{(\Delta x)^2}{12} \tag{5}$$

It is interesting to note this is the variance of an uniform distribution of width Δx; in fact the distribution of position error inside a pixel is uniform. A large under-sampling (perturbing the zero frequency) adds more complex terms that grow up the variance (with $\Re(z)$ is the real part of the complex z):

$$\mathrm{Var}(\varepsilon_{\mathrm{sampling}}) = \frac{(\Delta x)^2}{12} + \frac{\Delta x}{\pi^2} \sum_{k>0} \frac{(-1)^{k+1}}{k} \Re\left(\hat{f}'(\frac{k}{\Delta x})\right) - \frac{\Delta x^2}{\pi^2} \sum_{k>0} \frac{(-1)^{k+1}}{k^2} \Re\left(\hat{f}(\frac{k}{\Delta x})\right) \tag{6}$$

*For example a pure coma image have a non-nil center of gravity even there is no tilt at all

This error must be taking into account when photon noise estimation is done; the photon position second order momentum is increased by adding the $Var(\varepsilon_{sampling})$. In the case of MaTilD experiment, the total number of photons per wavelength is $\simeq 10^6$, and the second order momentum of image is $\simeq 64$ pixel^2. Combined effect of photon and sampling noises gives an error with a standard deviation error $\simeq 6 - 20\ 10^{-3}$ pixel.

3.1.3. Effect of an additive noise

By additive noise we consider every noises independent of the signal; the most important is the CCD readout noise, but is also present the noise due to thermal charge generation and the sampling error in intensity due to the finite number of sampling level. Without lost of generality lets consider a centered additive noise characterized by a standard deviation σ_{add}. Then the estimation of the center of gravity x_0 in a $M \times M$ pixels window is biased by:

$$\text{B}_{\text{add}} = x_0 M^2 \frac{\sigma_{\text{add}}^2}{N_{ph}^2} - \frac{\sigma_{\text{add}}^2}{N_{ph}^2} \sum_i^M i\Delta x \tag{7}$$

This bias can be minimized by choosing a window centered on x_0. Therefore The sum of $i\Delta x$, taken between $-M/2$ and $M/2$, is null. Then $x_0 \leq \Delta x/2$ and the bias is less than:

$$\text{B}_{\text{add}} \leq M^2 \frac{\Delta x \sigma_{\text{add}}^2}{2N_{ph}^2} \tag{8}$$

In the case of MaTilD experiment, the window size is $\simeq$100 pixels (to limit the windowing error), so the bias is less than: $0.02\ 10^{-6}$ pixel and is negligible compared to other noises.

Assuming the computation window is centered on the center of gravity, we can derived the variance the error:

$$\text{Var}(\varepsilon_{\text{add}}) = x_0^2 2M^2 \frac{\sigma_{\text{add}}^2}{N_{ph}^2} + \frac{M^2(M^2-1)(\Delta x)^2}{12N_{ph}^2}\sigma_{\text{add}}^2 \tag{9}$$

In MaTilD experiment, this gives an additive noise standard deviation $\simeq 5 - 10\ 10^{-3}$, this is less or equal to photon noise. We see the window size is very important because this variance varies as M^4. But as we will see in the following there is a trade-off between the additive noise and the error due to windowing which is larger as the window is smaller.

3.1.4. Simulation: effect for windowing and overlapping

Here we consider non-linear effects which depend on turbulence and on the experience. The first one is the image windowing due, in detection process, to the finite size of detector and, in data processing, to the computation window. In case of centro-symmetric images, this effect is null because the forgotten signal will not change the position of the center of gravity. But in the non symmetric image case, the windowing induces a bias. This bias leads to underestimate the center of gravity and depends on image pattern. Because it is different from image to image, a solution to study this phenomena is to make simulation with turbulence modeled by a Kolmogorov phase screen. Its characteristics like r_0 or the smallest pattern (related to the inner scale) are deduced from the experiment. The simulation was done for 200 phase screens. The result is that the windowing bias is as important as the other noises with a standard deviation $\simeq 10 - 20\ 10^{-3}$ pixels. This bias could be reduce by increasing the window size but then additive noise grows rapidly and the second non-linear effect too: the overlapping of image on the detector. The origin of this effect is that the wing of a monochromatic image pattern is added to the flux from other wavelength images, biasing also the center of gravity. So there is a trade off than could be made, but the gain in term of precision is not significant on MaTilD experiment (the optimal window size is between 100 and 150 pixels depending on the wavelength).

This study allow us to predict the signal to noise ratio for the MaTilD experiment in case of centroiding. The final precision on measurements is $\simeq 20 - 30\ 10^{-3}$ pixel and the differential tilt between the different wavelengths is $\simeq 30 - 120\ 10^{-3}$, its gives a signal to noise ration of 6. A typical correlation between the tilt and the differential tilt is shown in figure 4

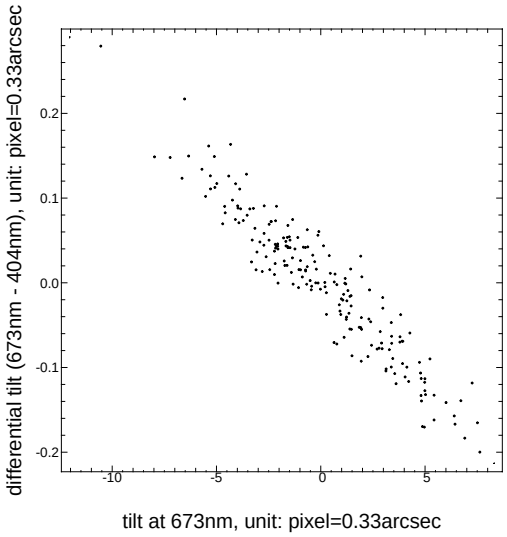

Figure 4. Correlation between differential tilt (673nm-404nm) and tilt (at 673nm). This correlation is obtain by using 200 simulations of MaTilD like images, including all the noise sources previously studied.

3.2. Fitting phase screen model

The tilt measured by centroiding makes no assumption about the shape of the images. We expect a noticeable improvement if a suitable model can be fitted onto the data. In MaTilD experiment, the observed brightness distribution $d_{\mathbf{x}}$ is the (incoherent) superposition of monochromatic PSF's plus some noise, hence the model:

$$m_{\mathbf{x}} = \sum_{\lambda} \alpha_{\lambda} \, |a_{\lambda,\mathbf{x}}|^2 \tag{10}$$

where $\mathbf{x}$ is the 2D position in the sampled image, the $\alpha_{\lambda} \geq 0$ are the intensities and the $a_{\lambda,\mathbf{x}}$ are the normalized complex amplitudes in the image plane which are the (backward) discrete Fourier transform (DFT) of the complex amplitude $\hat{a}_{\lambda,\mathbf{u}}$ in the pupil plane:

$$a_{\lambda,\mathbf{x}} = \sum_{\mathbf{u}} F_{\mathbf{x},\mathbf{u}} \, \hat{a}_{\lambda,\mathbf{u}} \quad \text{with} \quad F_{\mathbf{x},\mathbf{u}} = \mathrm{e}^{+\mathrm{i}2\pi \mathbf{x}\cdot\mathbf{u}/M} \tag{11}$$

where M is the number of pixels per image side. Assuming that the pupil-plane amplitude is due to a phase screen $\varphi_{\lambda,\mathbf{u}}$ over the pupil $p_{\lambda,\mathbf{u}}$, holds:

$$\hat{a}_{\lambda,\mathbf{u}} = p_{\lambda,\mathbf{u}} \mathrm{e}^{\mathrm{i}\varphi_{\lambda,\mathbf{u}}} \tag{12}$$

the phase in the pupil can be approximated by its expansion onto a finite basis of functions, e.g. the Zernike polynomials, $\{B_k(\mathbf{r}); k = 1..N_{\mathrm{basis}}\}$ where $\mathbf{r} = \lambda\mathbf{u}$ is the position in the pupil:

$$\varphi_{\lambda,\mathbf{u}} = \beta_{\lambda} \sum_{k=1}^{N_{\mathrm{basis}}} c_{k,\lambda} b_{k,\lambda,\mathbf{u}} \tag{13}$$

with $b_{k,\lambda,\mathbf{u}} = B_k(\lambda\mathbf{u})$ and where $\beta_{\lambda} \propto (n_{\lambda} - 1)/\lambda$ and where the $c_{k,\lambda}$ are coefficients of the expansion.

As it is customary done, we obtain the parameters of the model by minimizing the likelihood term of the data $d_{\mathbf{x}}$ with respect to the model $m_{\mathbf{x}}$:

$$L(\mathbf{d}|\mathbf{m}) = \sum_{\mathbf{x}} w_{\mathbf{x}} [d_{\mathbf{x}} - m_{\mathbf{x}}]^2 \quad \text{with} \quad w_{\mathbf{x}} = \begin{cases} 1/\mathrm{Var}(d_{\mathbf{x}}) & \text{where data is available} \\ 0 & \text{elsewhere} \end{cases} \tag{14}$$

flux (counts)	10^4	10^5	10^6
number of simulations	100	100	500
RMS differential tilt error (pixels)			
centroid	0.311	0.0397	0.0103
$N_{\text{basis}} = 3$	0.033	0.0062	0.0055
$N_{\text{basis}} = 4$	0.032	0.0061	0.0053
$N_{\text{basis}} = 5$	0.034	0.0057	0.0049
$N_{\text{basis}} = 6$	0.037	0.0054	0.0047
$N_{\text{basis}} = 7$	0.042	0.0056	0.0047
$N_{\text{basis}} = 8$	0.046	0.0047	0.0044
$N_{\text{basis}} = 9$	0.050	0.0052	0.0044

Table 1. Precision for the measured differential tilt by different methods: the center of gravity method (first line named "centroid") and the fit of a phase screen model (following lines).

We used a *modified* Newton algorithm to fit the phase coefficients. Since the likelihood quadratically depends on the intensities α_λ, the best set of intensities at every iteration can be directly obtained by least square fit (which involves a single matrix inversion). We choose the basis of functions such that the phase tilt is uniquely given by the 2 first modes $B_1(\mathbf{r})$ and $B_2(\mathbf{r})$. With this property, in the polychromatic case, all the $c_{k,\lambda}$ but the 2 first ones (i.e. the tilt) becomes identical (i.e. same optical path perturbation) for all wavelengths.

In order to compare the centroid and phase fit methods, we measured the differential tilt from 2 independent monochromatic realizations with brightness distributions $I(\mathbf{x})$ and $I(\mathbf{x} - \Delta\mathbf{x})$ respectively (i.e. same total flux, and same Kolmogorov phase screen except by a slight tilt $\propto \Delta\mathbf{x}$). In our simulations, the image size was 64×64, the pupil diameter was 31 *frequels* (i.e. Shannon sampling) with a central obstruction of 1/3; random turbulent phase screens with $D/r_0 = 4$ were used, the additive background noise level was 2 counts RMS, and we varied the total flux and the number of modes N_{basis}. Comparison between different measurement of differential tilt are summarized in Table 1. The phase fit method appears to improve the estimate of the differential tilt by a factor greater than 2 at high fluxes (10^6 counts) and up to a factor of almost 10 at low fluxes (10^4 counts).

The number N_{basis} of modes is a means to tune the regularization level of the inverse problem of obtaining the model from the data: with too many modes, the model will fit noise artifacts; on the contrary with too few modes, the model will be unable to fit true phase aberrations. In other words, we expect the best performances with the phase fit method for a suitable number of modes which should depends on incoming flux and background noise level. This behavior can be seen in Table 1.

4. CONCLUSION: FROM SIMULATIONS TO DATA

As shown by simulation, the differential tilt can be measured on data; with a better reliability for phase map fitting. Up to day, the processing of real data does not yet give the result attempted from simulations. But there is some possible sources of noise that haven't been considered, like error in flat field correction or inhomogeneity of sensitivity inside pixel. But a qualitative estimation show they won't be significant, so the demonstration of measurabilty of differential tilt would be done in a very short future.

ACKNOWLEDGMENTS

We are most grateful to the technical staff at the Observatoire de Lyon for their help. The work has been done with the support of the CNRS/PNHRA, the Région Rhones-Alpes contract L14840.00.00/97018030 and the CNRS/Ultimatech.

REFERENCES

1. R. Foy, A. Migus, F. Biraben, G. Grynberg, P. R. McCullough, and M. Tallon, "The polychromatic artificial sodium star: A mew concept for correcting the atmospheric tilt," *Astronomy and Astrophysics, Supplement Series* **111**, pp. 569–578, June 1995.

2. M. Séchaud, N. Hubin, L. Brixon, R. Jalin, R. Foy, and M. Tallon, "Laser Backscattered Reference Star for Atmospheric Wavefront Disturbances Measurement," in *Very Large Telescopes and their Instrumentation*, U. M.-H., ed., ESO/NOAO Conferences, pp. 705–714, ESO, (Garching, Germany), 1988.
3. F. Rigaut and E. Gendron, "Laser guide star in adaptive optics: the tilt determination problem," *Astronomy and Astrophysics* **261**, pp. 677–684, 1992.
4. M. Le Louarn, N. N. Hubin, R. Foy, and M. Tallon, "Sky coverage and psf shape with lgs ao on 8-m telescopes," *Proceding SPIE* **3353**, pp. 364–370, Sept. 1998.
5. R. Ragazzoni, S. Esposito, and E. Marchetti, "Auxiliary telescopes for the absolute tip-tilt determination of a laser guide star," *Monthly Notices of the Royal Astronomical Society* **276**, pp. L76–L78, Oct. 1995.
6. R. Ragazzoni, "propagation delay of a laser beacon as a tool to retrieve absolute tilt measurements," *The Astrophysical Journal* **465**, pp. 73–75, July 1996.
7. R. Ragazzoni and E. Marchetti, "Further techniques for lgs tilt recovery: the perspective and the predictive approach," *Proceding SPIE* **2871**, pp. 948–952, Mar. 1997.
8. M. Schöck, R. Foy, J.-P. Pique, P. Chevrou, N. Ageorges, A. Petit, V. Bellanger, H. Fews, F.-C. Foy, C. Högemann, M. Laubscher, O. Peillet, P. Segonds, M. Tallon, and J.-M. Weulersse, "Pass-2: Quantitive measurements of the polychromatic laser guide star," in *in this proceedings*, SPIE, 2000.
9. D. L. Fried, "optical resolution through a randomly inhomogeneous maedium for very long and very short exposures," *Journal of Optical Society of America* **56**, 1996.
10. a. Tokovinin, "Pendular seismometer for correcting telescope pointing errors," in *in this proceedings*, SPIE, 2000.
11. C. W. Allen, *Astrophysical Quantities*, The Athlone Press, University of London, 1976.
12. V. I. Tatarskii, *The effects of the turbulent atmosphere on wave propagation*, Jerusalem: Israel Program for Scientific Translations, 1971, 1971.
13. J. C. Fontanella, "Analyse de surface d'onde, déconvolution et optique active," *Journal of Optics* **16**, 1985.